14th World Congress in Computational Mechanics (WCCM)
ECCOMAS Congress 2020
Virtual Congress: 11 – 15 January 2021
F. Chinesta, R. Abgrall, O. Allix and M. Kaliske (Eds)

THE DKMQ-SS SOLID SHELL ELEMENT: FORMULATION ASPECTS AND APPLICATIONS

J.L. BATOZ[1], S. BOUABDALLAH[2], S. SOELARSO[3], E. ANTALUCA[3], F. LAMARQUE[3]

[1] Sorbonne Universités-Université de Technologie de Compiègne UMR 7337, 60200 Compiègne, France, batoz@utc.fr

[2] UTeam – Université de Technologie de Compiègne, 60200 Compiègne, France, salim.bouabdallah@free.fr

[3] Sorbonne Universités-Université de Technologie de Compiègne EA7284, 60200 Compiègne, France, soelarso.soelarso@utc.fr, eduard.antaluca@utc.fr, fabien.lamarque@utc.fr

Key words: Solid-Shell formulation, 8 nodes Hexahedral element, DKMQ plate element, shallow foundation system.

Abstract. In this paper we present the formulation of a solid-shell element with 24 dof (the three cartesian components of displacement at the eight nodes of a solid hexahedron element), taking into account previous contributions to avoid shear, trapezoidal and thickness locking. But we also enhance the 3D displacement field by incomplete quadratic terms to improve the bending and transverse shear energies as was done for the performing DKMQ plate bending element proposed by Katili. After the formulation aspects, we present the results for some classical benchmark problems and for the linear analysis of a particular shallow foundation system called "spider net system footing" used in Indonesia.

1 INTRODUCTION

Since 1985 a significant number of researchers have contributed to the development of finite element models (FEM) for the analysis of shell type structures (situation where one dimension, the thickness, is smaller than the two other characteristics of the middle surface), where the dofs are only the nodal displacements, and without using generalized stress and strain resultants quantities. Those FEM are called Solid-Shell elements, mainly based on 8 nodes brick (hexahedron) and 6 nodes prism elements. The displacements are linear through the thickness (as in the "first order shell theories"), but 3D constitutive (stress-strain) relations can be considered if the strain field is enhanced at the element level. Compared to the formulation of classical 3D solid elements, the formulation involves a strain description in local orthogonal curvilinear coordinates where the thickness direction plays a particular role (as in shell theories) in order to take into account the existing knowledge of performing shell FEM (for example to avoid shear locking for thin plates and shells). Additional modifications are needed to obtain efficient elements in various situations (thin to thick bodies, representation of curved geometries) but the solid-shell elements allow efficient non-linear geometrical analysis, modeling of complicated geometries with stiffeners and branches,

modeling of soil structure and fluid structure interactions due to the direct possibility of surface contact between domains and nodal variables compatibility.

We will not propose an exhaustive review of publications dealing with the development of Solid-Shell (SS) elements, and we will restrict our discussions to hexahedron (H8) elements. Most of the elements are sharing the same theoretical aspects: C° continuity of the geometry, linear variation through the thickness, assumed natural strains (ANS) for transverse shear to avoid shear locking, linear variation of the normal strain to use full 3D stress strain relations to avoid Poisson thickness locking, enhanced normal strain distribution in curved geometries to avoid curvature trapezoidal locking [12-13]. The H8-SS elements found in the literature differ by their detailed formulation aspects and target applications (like linear or non-linear analysis, static or dynamic analysis, etc), see [5-13] among others between 2000 and 2020.

In the present paper we propose the development of two H8 solid-shell elements, with classical (known) modifications avoiding shear locking and trapezoidal locking and with enhanced normal thickness strain for full use of the 3D constitutive relations. The first element can be viewed as a 3D extension of the so-called MITC4 shell element [1], (also called Q4γ24 in [2]), therefore we call the new solid-shell element MITC4-SS. The second element is a modification of the previous one taking into account the formulation of the DKMQ plate/shell element [3]. The comparison between MITC4 and DKMQ plate bending element was done in [4]. These two elements are quite easy to program, without adjusting parameters and were found to be both precise and efficient for plate and shell analysis. After the formulation aspects presented in section 2, we present some numerical results for classical linear benchmark tests.

2 GENERAL SPECIFICATIONS

2.1 Geometry

The DKMQ-SS element is based on the classical isoparametric 8 nodes brick element. Hence the position vector at any point q is given by (figure 1):

$$\vec{x}_q(\xi,\eta,\zeta) = \vec{x}_p(\xi,\eta) + \zeta\ \vec{V} = \sum_{i=1}^{k} N_i(\xi,\eta)\left[\frac{1-\zeta}{2}\vec{x}_i^- + \frac{1+\zeta}{2}\vec{x}_i^+\right] \tag{1}$$

$-1 \le \xi,\eta,\zeta \le 1$ 2D reference coordinates ; ζ thickness reference coordinate

and $N_i = \frac{1}{4}(1+\xi_i\xi)(1+\eta_i\eta)$

$\vec{X}_i^+$ and $\vec{X}_i^-$ coordinates of the top $(+)$and bottom nodes$(-)$.

$\vec{V}_i = \vec{X}_i^+ - \vec{X}_i^-$ thickness (director or fiber) vectors

From equation 1, we can define the covariant basis vectors $\vec{a}_{i\zeta}$ at any point q (figure 2):

$$d\vec{x}_q = \vec{a}_{1\zeta}d\xi + \vec{a}_{2\zeta}d\eta + \vec{a}_{3\zeta}d\zeta$$

and the gradient coordinate tensor $[F_\zeta]$:

$$\{dx_q\} = [F_\zeta]\ \{d\xi\} \qquad [F_\zeta] = [\vec{a}_{1\zeta}\quad \vec{a}_{2\zeta}\quad \vec{a}_{3\zeta}] \tag{2}$$

$$\langle d\xi \rangle = \langle d\xi\ \ d\eta\ \ d\zeta \rangle$$

An orthogonal curvilinear basis defined by matrix $[Q_\zeta]$ can be defined such that:

$$\{d\vec{x}_q\} = [Q_\zeta]\{dx_{qt}\} \quad with \quad [Q_\zeta] = [\overrightarrow{t_{1\zeta}} \quad \overrightarrow{t_{2\zeta}} \quad \overrightarrow{n_\zeta}] \quad and. \quad \overrightarrow{t_{1\zeta}} = \frac{\overrightarrow{a_{1\zeta}}}{|\overrightarrow{a_{1\zeta}}|} \tag{3}$$

$$\text{with } \overrightarrow{n_\zeta} = \frac{\overrightarrow{a_{1\zeta}} \wedge \overrightarrow{a_{2\zeta}}}{|\overrightarrow{a_{1\zeta}} \wedge \overrightarrow{a_{2\zeta}}|}$$

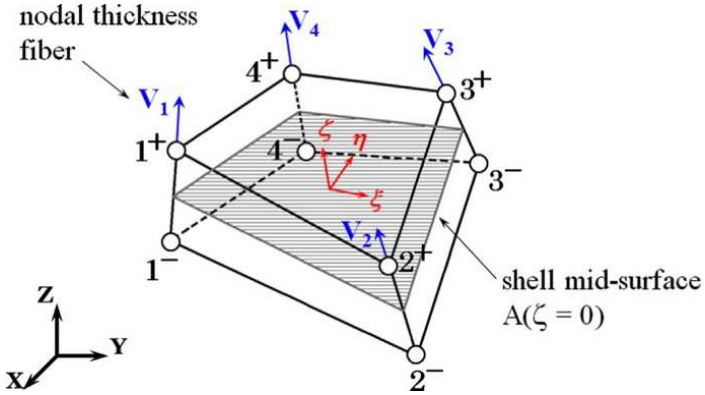

Figure 1: Geometry of the 8 nodes solid-shell DKMQ-SS element.

The local coordinates are x, y, z' (figure 2), so that: $\langle dx_{qt} \rangle = \langle dx\ dy\ dz' \rangle$

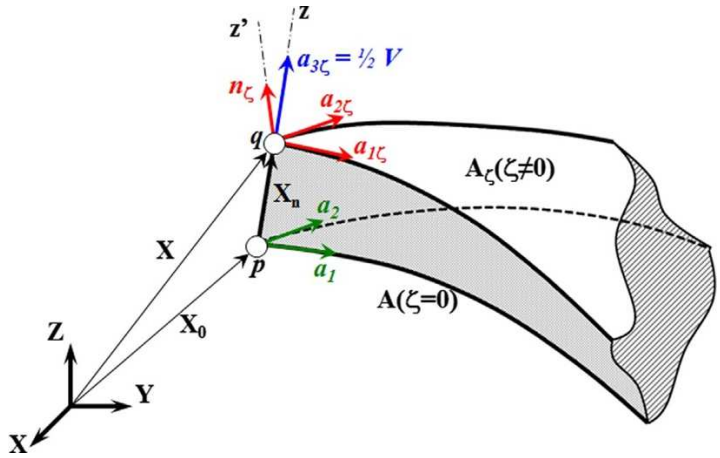

Figure 2. Covariant basis vectors at point q and coordinate z'.

Hence the derivatives of f with respect to the local orthogonal directions x, y, z' are:

$$\left\{\frac{\partial f}{\partial x_{qt}}\right\} = [C_\zeta]^T \left\{\frac{\partial f}{\partial \xi}\right\} \quad \text{or.} \quad \{d\xi\} = [C_\zeta]\{dx_{qt}\} \quad \text{with.} \quad [C_\zeta] = [F_\zeta]^{-1}[Q_\zeta] \tag{4}$$

2.2 3D Displacement field

For a "conventional H8 solid-shell element", here called MITC4-SS element, the displacement field is given by:

$$\vec{u}_q = \sum_{i=1}^{4} N_i \left(\vec{u}_{pi} + \zeta \Delta\vec{u}_{qi}\right)$$

$$\text{with} \quad \vec{u}_{pi} = \tfrac{1}{2}\left(\vec{u}^+_{qi} + \vec{u}^-_{qi}\right) \quad \text{and} \quad \overrightarrow{\Delta u}_{qi} = \tfrac{1}{2}\left(\vec{u}^+_{qi} - \vec{u}^-_{qi}\right) \tag{5a}$$

The nodal displacements at the upper and lower nodes are U, V and W along X, Y, Z in a global cartesian coordinate system. We can define the 24 components nodal displacement vector as U, V, W at nodes -1, -2, -3, -4, 1, 2, 3, 4 (figures 1 and 3):

$$\langle u_n \rangle = \langle \ (U_{-i}\, V_{-i}\, W_{-i}) \ i = 1{,}4 \quad (U_{+i}\, V_{+i}\, W_{+i}\,) \ i = 1{,}4 \,\rangle = \langle \ U_i\, V_i\, W_i \ \ i = 1{,}8 \rangle \quad (5b)$$

$\vec{u}_{pi}$ are the mid surfaces displacements and $\overrightarrow{\Delta u_{qi}}$ are the increments of displacements at ζ=1.
$\vec{u}^{+}_{qi}$ are the nodal displacements U^+, V^+, W^+ at the node i on the upper surface ζ=1;
$\vec{u}^{-}_{qi}$ are the nodal displacements U^-, V^-, W^- at the node i on the lower surface ζ=-1.

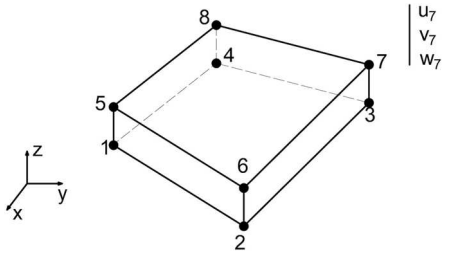

Figure 3. Nodal variables of the solid-shell element MITC4-SS and DKMQ-SS.

For the present DKMQ-SS element, the 3D displacement field is enhanced by 4 parameters $\Delta\beta_k$ defined at the lateral faces and by 4 quadratic interpolation fonctions P_k. The above proposal is in agreement with the formulation of the DKMQ element [3, 4]:

$$\vec{u}_q = \sum_{i=1}^{4} N_i \left(\vec{u}_{pi} + \zeta\, \Delta\vec{u}_{qi}\right) + \sum_{k=5}^{8} P_k \left(\tfrac{1}{2}\widetilde{h_k}\right) \zeta\, \Delta\beta_k\, \vec{t}_k \qquad (6)$$

$\tilde{h}_k$ is the thickness at node k. $\vec{t}_k$ is the unit tangent vector along the side k between corner nodes i and j on the mid surface $\zeta = 0$. We can define the four components vector

$$\langle \Delta\beta_n \rangle = \langle \Delta\beta_5 \quad \Delta\beta_6 \quad \Delta\beta_7 \quad \Delta\beta_8 \rangle \qquad (7)$$

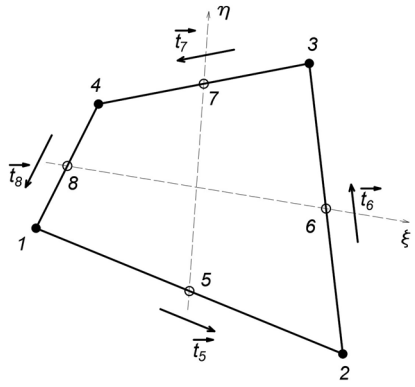

Figure 4. Mid surface ζ=0 and mid-points 5, 6, 7, 8.

The quadratic functions P_k are:

$$P_k = \tfrac{1}{4}(1-\xi^2)(1+\eta_k\,\eta) \ \text{ for } k = 5,7 \text{ and } P_k = \tfrac{1}{4}(1-\eta^2)(1+\xi_k\,\xi) \ \text{ for } k = 6,\ 8$$

2.3 Displacement gradients, strains and stresses

The cartesian displacement gradients are obtained using equations 1 to 5:

$$\{d\vec{u}_q\} = [L]\{\vec{x}_q\} \quad \text{with} \quad [L] = [L_\zeta][F_\zeta]^{-1} \quad \text{and} \quad [L_\zeta] = [\vec{u}_{q,\xi} \;\; \vec{u}_{q,\eta} \;\; \vec{u}_{q,\zeta}] \tag{8}$$

The curvilinear displacement gradients are:

$$\{d\vec{u}_q\}_t = [L_t]\{d\vec{x}_{qt}\} \quad \text{with} \quad [L_t] = [Q_\zeta]^T[L_\zeta][C_\zeta] \tag{9}$$

with $[L_\zeta] = [\vec{u}_{q,\xi} \;\; \vec{u}_{q,\eta} \;\; \vec{u}_{q,\zeta}]$

From the above we can define the curvilinear strain components:

$$\langle \mathcal{E}_t \rangle = \langle \langle \mathcal{E}_s \rangle \;\; \mathcal{E}_{z'} \;\; \langle \underline{\gamma}_s \rangle \rangle \tag{10}$$

with the in-plane strains: $\langle \mathcal{E}_s \rangle = \langle \varepsilon_{xx} \;\; \varepsilon_{yy} \;\; \gamma_{xy} \rangle$
the normal thickness strain: $\mathcal{E}_{z'}$ with z' along $\vec{n_\zeta}$
the *assumed independent* transverse shear strains are defined simply as: $\langle \underline{\gamma}_s \rangle$

The local conjugate curvilinear stresses components are:

$$\langle \sigma_t \rangle = \langle \langle \sigma_s \rangle \;\; \sigma_{z'z'} \;\; \langle \tau_s \rangle \rangle \tag{11}$$

with the in-plane stresses: $\langle \sigma_s \rangle = \langle \sigma_{xx} \;\; \sigma_{yy} \;\; \sigma_{xy} \rangle$
the normal thickness stress: $\sigma_{z'z'}$
the transverse shear stresses: $\langle \tau_s \rangle = \langle \sigma_{xz'} \;\; \sigma_{yz'} \rangle$

2.4. Internal virtual work expressions

The internal virtual work on an element is thus given by:

$$W_{int}^e = \int_V \langle \delta\varepsilon_t \rangle \{\sigma_t\}\, dV = \int_V \langle \delta\varepsilon_s \rangle \{\sigma_s\}\, dV + \int_V \delta\varepsilon_{z'}\, \sigma_{z'z'}\, dV + \int_V \langle \delta\underline{\gamma}_s \rangle \{\tau_s\}\, dV.$$

$$W_{int}^e = W_{int}^{mb} + W_{int}^{\varepsilon z} + W_{int}^{s} \tag{12}$$

the first term is the membrane-bending internal work contribution (mb superscript), the second term is the thickness stress-strain contribution and the third term is the transverse shear contribution.
We consider here 3D constitutive relations for linear elasticity represented in a matrix form using the 6x6 symmetric matrix $[H]$ such that:

$$\{\sigma_t\} = [H]\{\varepsilon_t\} \tag{13}$$

In the case of isotropy, we can partition matrix $[H]$ and define sub-matrices $[H_1]$ (3x3), $[H_2]$ (3x3) and $[G]$ (2x2) such that:

$$\{\sigma_s\} = [H_1]\{\varepsilon_s\}\,; \{\sigma_z\} = [H_2]\{\varepsilon_{z'}\}\,;$$
$$\{\tau_s\} = [G]\left\{\underline{\gamma}_s\right\}\,; \langle \varepsilon_z \rangle = \langle \varepsilon_{xx} \;\; \varepsilon_{yy} \;\; \varepsilon_{z'} \rangle$$

$$\langle \sigma_z \rangle = \langle \sigma_{xx} \;\; \sigma_{yy} \;\; \sigma_{z'z'} \rangle$$

and

$$[H_1] = a \begin{bmatrix} 1-\nu & \nu & 0 \\ \nu & 1-\nu & 0 \\ 0 & 0 & \frac{1-2\nu}{2} \end{bmatrix} ; \; [H_2] = a \begin{bmatrix} 0 & 0 & \nu \\ 0 & 0 & \nu \\ \nu & \nu & 1-\nu \end{bmatrix} ; \quad [G] = G \begin{bmatrix} 1 & 0 \\ 0 & 1 \end{bmatrix} \qquad (14)$$

with $a = \frac{E}{(1+\nu)(1-2\,\nu)}$ and. $G = \frac{E}{2\,(1+\nu)}$

With these constitutive equations, the different contributions of the internal virtual works can be written as:

$$W_{int}^{mb} = \int_V \langle \delta\varepsilon_s \rangle [H_1] \{\varepsilon_s\} \, dV; \qquad W_{int}^{\varepsilon z} \int_V \langle \delta\varepsilon_{z'} \rangle [H_1] \{\varepsilon_{z'}\} \, dV; \qquad W_{int}^{s} \int_V \langle \delta\underline{\gamma}_s \rangle [H_1] \left\{\underline{\gamma}_s\right\} dV \qquad (15)$$

2.5. Enhancement of the normal thickness strains

For proper use of the 3D constitutive equations and possibility to converge to the plane stress solution in bending for any Poisson coefficient, the thickness normal strains must be enriched by a linear term in ζ [13]:

$$\varepsilon_{z'}^{Enr} = \varepsilon_{z'} + \alpha \, \zeta. \qquad (16)$$

where α is an independent internal parameter.

The remedy to avoid *trapezoidal locking* when the thickness vectors $\vec{V}_i$ are not parallel, is to modify (enhance) the definition of the thickness strain using a bilinear interpolation in terms of the thickness strain values at the four vertices on the mid surface:

$$\varepsilon_{z'}^{EAS}(\xi, \eta) = \sum_{i=1}^{4} N_i \, (\xi, \eta) \quad \varepsilon_{z'}(\xi_i, \, \eta_i) \qquad (17)$$

2.6. Assumed transverse shear strains

The transverse shear strains are assumed constant through the thickness. Therefore, the shear strains on the mid-surface are $\gamma_{xz}\,(\xi, \eta)$ and $\gamma_{yz}\,(\xi, \eta)$. To avoid *transverse shear locking* we adopt the method of assumed natural strain of the MITC4 element where the covariant shear strain $\gamma_{\xi\zeta}$ is linear in η and $\gamma_{\eta\zeta}$ is linear in ξ. The cartesian components of transverse shear strains are then given by [1-4] (figure 5):

$$\{\gamma_s\} = \begin{Bmatrix} \gamma_{xz} \\ \gamma_{yz} \end{Bmatrix} = [cj] \, [N_\gamma] \{\gamma_{sn}\} \qquad (18)$$

with $$[N_\gamma] = \frac{1}{8} \begin{bmatrix} (1-\eta)\, h_5 L_5 & 0 & -(1+\eta)\, h_7 L_7 & 0 \\ 0 & (1+\xi)\, h_6 L_6 & 0 & -(1-\xi)\, h_8 L_8 \end{bmatrix}$$

$$\langle \gamma_{sn} \rangle = \langle \gamma_{sz}^{12} \;\; \gamma_{sz}^{23} \;\; \gamma_{sz}^{34} \;\; \gamma_{sz}^{41} \rangle = \langle \gamma_5 \;\; \gamma_6 \;\; \gamma_7 \;\; \gamma_8 \rangle \qquad (19)$$

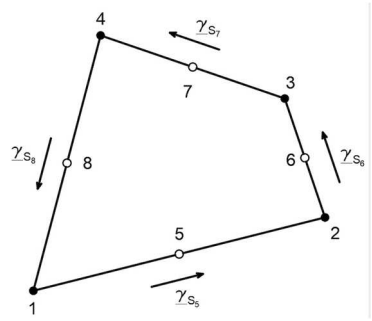

Figure 5: Shear strains on sides

$[cj]$ is a 2x2 matrix involving the components of $[C_\zeta]$ for $\zeta = 0$. $L_5 = L_{12}$; $L_6 = L_{23}$; $L_7 = L_{34}$; $L_8 = L_{41}$; L_{ij} is the length of side ij. h_5 is the thickness at node 5, etc. The constant values $\gamma_{sz}^{ij} = \gamma_k$ are obained considering :

$$\gamma_k = \frac{1}{L_k} \int_0^{L_k} \gamma_{sz}\, ds \qquad \text{with} \quad \gamma_s = \vec{u}_{p,s}\, \vec{n} + \frac{1}{h} \Delta\vec{u}_{q,z}\, \vec{t}_k$$

Leading to:

$$\gamma_k = \frac{1}{L_k}\left(\vec{u}_{pj}\ \vec{n}_j - \vec{u}_{pi}\ \vec{n}_i\right) + \frac{1}{2h}\left(\Delta\vec{u}_{qi} + \Delta\vec{u}_{qj}\right)\vec{t}_k + \frac{2}{3}\Delta\beta_k \tag{20}$$

2.7. Independent transverse shear strains

As in the DKMQ element [3-4], the assumed independent transverse shear $\langle \underline{\gamma}_s \rangle$ are chosen as four constant shear strains on the sides on the middle surface $\zeta = 0$, taking into account local static equilibrium with incomplete expressions of the shear force T_s and bending moment M_s. If the displacement field includes quadratic terms as in equation 6, then we obtain on each side ij:

$$\underline{\gamma}_k = \frac{D_b}{D_s}\, \beta_{,ss} = -\frac{2}{3}\, \phi_k\, \Delta\beta_k \qquad \text{with.} \quad \phi_k = \frac{D_b}{D_s}\, \frac{12}{L_k^2} = \frac{2}{k\,(1-\nu)}\, \frac{h^2}{L_k^2} \tag{21a}$$

where $D_b = \frac{12\, h^3}{1-\nu^2}$ and $D_s = \frac{kGh}{2(1+\nu)}$ k is the shear correction factor (=5/6).

Hence the independent shear strains are:

$$\left\{\underline{\gamma}_{sn}\right\} = [A_\phi]\{\Delta\beta_n\} = -\frac{2}{3}\begin{bmatrix} \phi_5 & 0 & 0 & 0 \\ 0 & \phi_6 & 0 & 0 \\ 0 & 0 & \phi_7 & 0 \\ 0 & 0 & 0 & \phi_8 \end{bmatrix}\{\Delta\beta_n\} \tag{21b}$$

$$\langle \Delta\beta_n \rangle = \langle \Delta\beta_5 \quad \Delta\beta_6 \quad \Delta\beta_7 \quad \Delta\beta_8 \rangle$$

2.8. Elimination of the internal variables $\Delta\beta_k$

The link between the independent shear strain $\underline{\gamma}_k$ (eqs. 21a,b) and the constant assumed shear strain γ_k resulting from the displacement field (eq. 20) is simply the following:

$$\underline{\gamma}_k = \gamma_k \tag{22}$$

leading to:

$$-\frac{2}{3}\,\phi_k\,\Delta\beta_k = \frac{1}{L_k}\left(\vec{u}_{pj}\;\vec{n}_j\;-\;\vec{u}_{pi}\;\vec{n}_i\right) + \frac{1}{2h}\left(\Delta\vec{u}_{qi} + \Delta\vec{u}_{qj}\right)\vec{t}_k + \frac{2}{3}\Delta\beta_k \qquad (23)$$

or

$$\frac{1}{L_k}\left(\frac{\vec{U}_j^+ + \vec{U}_j^-}{2}\vec{n}_j - \frac{\vec{U}_i^+ + \vec{U}_i^-}{2}\vec{n}_i\right) + \frac{1}{2h_k}\left(\vec{U}_j^+ - \vec{U}_j^- + \vec{U}_i^+ - \vec{U}_i^-\right).\vec{t}_k + \frac{2}{3}(1+\phi_k)\,\Delta\beta_k = 0$$

The four variables $\Delta\beta_k$ for $k = 5,6,7,8$ can be then expressed in terms of the 24 nodal displacements U, V, W at the 8 nodes of the DKMQ-SS element:

$$\{\Delta\beta_n\} = [A]^{-1}[A_u]\{u_n\} \qquad \text{with } [A] = [I] - [A_\phi] \qquad (24)$$

$[A_u]$ is a 4 by 24 matrix in terms of L_5 to L_8, h_5 to h_8, the direction cosines of $\vec{n}_k$ at nodes 1 to 4 (of the middle surface) and the direction cosines of the tangent vectors $\vec{t}_k$ along mid side points.

2.9. Strain matrices

From the above expressions and considering the approximations of the 3D displacement field in terms of the element dof, vectors $\langle u_n \rangle$ and $\langle \Delta\beta_n \rangle$, we can define the strain matrices for the membrane and bending strains $[B_1]$ and $[B_2]$:

$$\{\varepsilon_s\} = [B_1(\xi,\eta,\zeta)]\{u_n\} + \{B_2(\xi,\eta)\}\{\Delta\beta_n\} \qquad (25a)$$

and using eq. 24 we can define:

$$\{\varepsilon_s\} = [B'_1(\xi,\eta,\zeta)]\{u_n\} \quad \text{with} \quad [B'_1] = [B_1] + \{B_2\}[A]^{-1}[A_u] \qquad (25b)$$

In terms of the nodal displacements and α parameter we can define the strain matrices $\langle B_3 \rangle$ and B_4 to define the thickness strain $\varepsilon_{z'}$ (eq. 17):

$$\varepsilon_{z'} = \langle B_3(\xi,\eta)\rangle\{u_n\} + B_4\,\alpha \qquad \text{with} \quad B_4 = \zeta. \qquad (26)$$

The transverse shear strains are given by equations 18, 20-24:

$$\{\gamma_s\} = \begin{Bmatrix}\gamma_{xz}\\ \gamma_{yz}\end{Bmatrix} = [B_5(\xi,\eta)]\{u_n\} \quad \text{with} \quad [B_5(\xi,\eta)] = [cj]\,[N_\gamma][A_\phi][A]^{-1}[A_u] \qquad (27)$$

Introducing equations 25 to 27 in the expression of the PVW (eq.15) we can define the elemnt stiffness matrix in terms of $\{u_n\}$ and α. The last internal dof can be eliminated by static condensation.

3 SOME NUMERICAL RESULTS

3.1. Classical benchmark tests

The stiffness matrix of the elements MITC4-SS or DKMQ-SS elements are both obtained using numerical integration considering a uniform 2x2x2 Gauss scheme leading to a proper rank of 18: no spurious modes and the evaluation of convergence rate can be done as usual by considering classical benchmark tests. We recall that the membrane performance of both elements should be the same. Regarding the behaviour in bending of plates, it was found in a recent comparative study [1] that DKMQ is slightly superior to MITC4 in s-norm tests for a large aspect ratio (from L/h= 2 to $10^{4)}$. The other improvements to avoid trapezoidal or thickness locking are the same in both MITC4-SS or DKMQ-SS hence the behaviour of both elements should be close in all tests we consider: square or circular plates, cylindrical panel

under self-weight (Scordelis-Lo), pinched cylinder with diaphragms, hemispherical shell with concentrated loads, helicoidal shells under concentrated loads for two length to thickness ratio. In all these tests we found overall very good results with small differences between the two elements. As an example, we present the convergence of the displacement under the load for the pinched cylinder (figure 6):

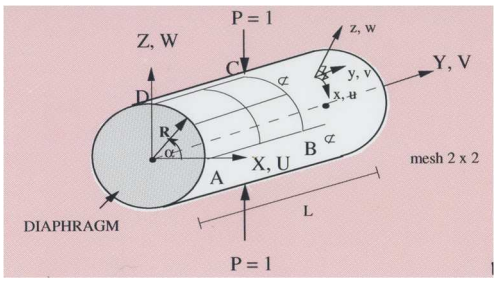

L=6m; R=3m; h=0.03m;
$\nu = 0.3$; E=3x10^{10} Pa
$U^+ = U^- = W^+ = W^- = 0$ on AD;
$U^+ = U^- = 0$ on CD ;
$V^+ = V^- = 0$ on BC
$W^+ = W^- = 0$ on AB
P= - 0.25 N at point C (for a quarter)

Figure 6 . Pinched cylinder

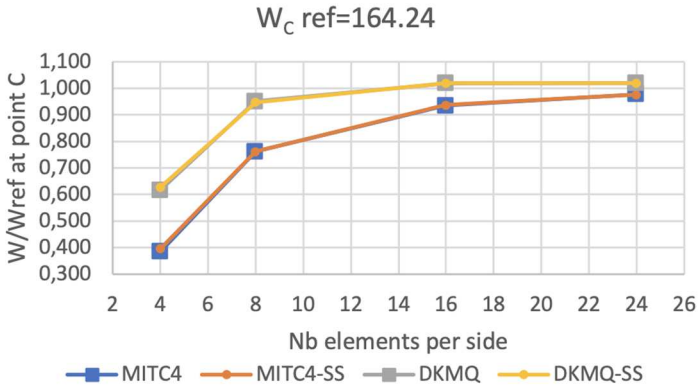

Figure 7. Convergence of displacement under the load using different elements

The results show a fast convergence for both MITC-SS and DKMQ-SS towards the reference solutions, with a slight superiority for the new element DKMQ-SS.

3.2. Application to the analysis of a shallow foundation cell

Figure 8 is related to a shallow foundation system called "Spider Net System Footing" (SNSF) used for many years in Indonesia for construction of 5 to 8 floors buildings on soft soil. The foundation results from the assemblage of cells made of vertical ribs with different orientations. Those ribs are supported by the natural soil. Columns are situated at the intersection of the different ribs. The cells are filled by soil material and compacted before closure with a reinforced slab.

Figure 9 shows a unit cell extracted from a real project. The horizontal dimensions of the slab are 8m by 7m with a thickness of 11 cm. The column of 5 m height with a square cross section 0.6mx0.6m is loaded on top by an horizontal force of 10 tons. The vertical ribs have a thickness of 10 cm and height of 1 m. We consider 4 external ribs and 4 internal ribs as shown. The cell is assumed simply supported on the natural soil level. On figure 9 we can see a typical mesh with H8 elements (N=8x8 on a quarter of the slab with 773 elements and 4264

dof). We consider only one element through the thickness. The column is also meshed with solid H8 elements. We assume linear elasticity with isotropy of the concrete structure.

Figure 8. The shallow foundation system called SNSF

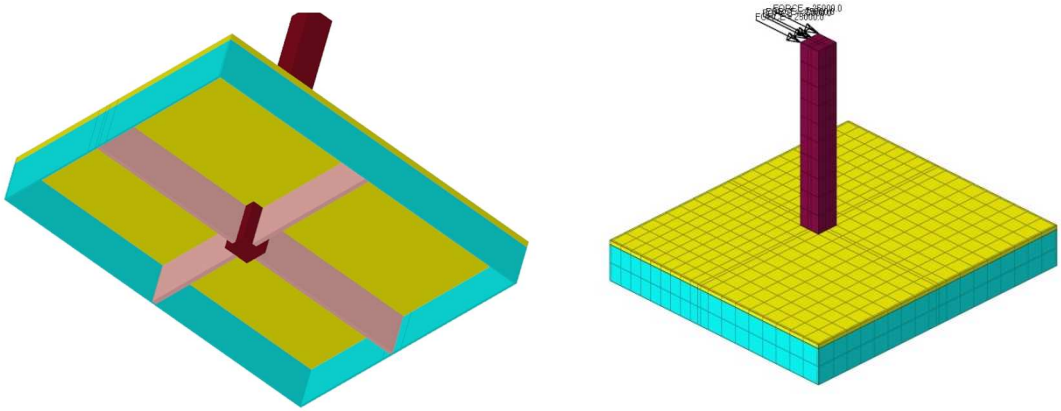

Figure 9 . 3D view of a unit cell and view of a mesh with around 770 H8 elements

On figure 10 we report the results of the horizontal displacement on top of the column considering different elements and for different meshes (obtained using Hypermesh [14]). The displacement due to the bending of the beam is 18 mm and the additionnal displacements are due to the flexibility of the SNSF cell (an increase of around 27 %). The results show that the best convergence rate is obtained using DKMQ-SS followed by MITC4-SS. They converge to the same value (around 23mm) as well as the SC8R element of Abaqus [5], a solid-shell element considering plane stress. We also report the results obtained with Optistruct [1]. They are the same as using the H8 solid element by Wilson and Taylor [2], based on quadratic incompatible modes. Those results are close to those of MITC4-SS and they are much better than those using the standard H8 solid element (Solid-H8 in the figure 10).

On figure 11 we show isovalues of principal stresses (P1 on left and P3 on right) for a fine mesh (N=16), for a view from below the structure. On the left (in red) we can identify a localized area with tensile stresses reaching 7.7 MPa and on the right an area (in blue) located in the lower part of a central rib with -7.7 MPa as max compression stresses.

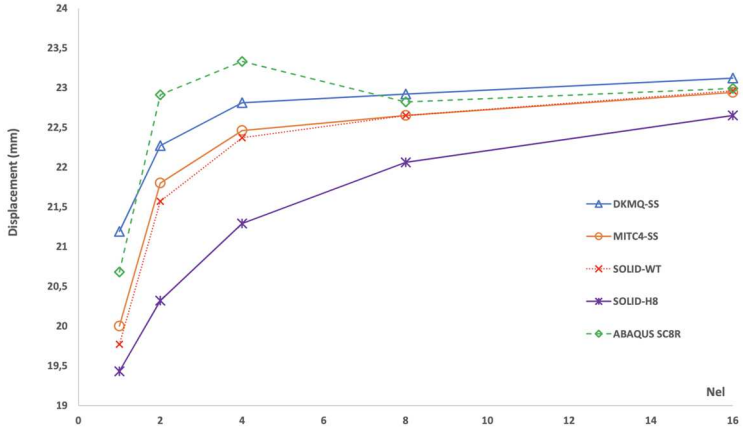

Figure 10. Convergence of the displacement under the load using different solid-shell elements.

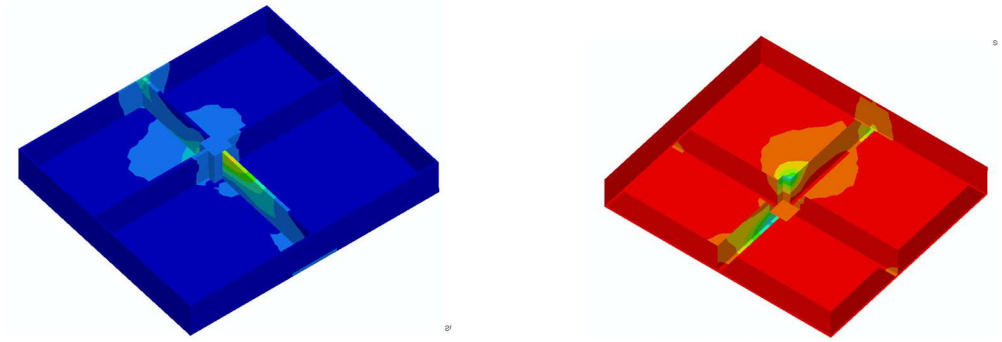

Figure 11. Isovalues of principal stresses.

4 CONCLUDING REMARKS

In this paper we present some formulation details regarding two solid shell elements, called MITC4-SS and DKMQ-SS with 8 nodes and 3 dof (the 3 cartesian components of displacements) per node. Their formulations have several aspects in common: trilinear lagrangian approximations of the geometry and of the 3D displacement field, modifications to avoid transverse shear and trapezoidal locking, enhancements of the thickness strain to avoid thickness locking and for use of 3D constitutive equations. The main contribution of the present paper concerns the DKMQ-SS element with the enhancement of the bending behaviour by quadratic terms in the spirit of the DKMQ plate element, aperforming element valid for very thick to very thin plates. After the formulation we present some numerical results regarding classical benchmark tests (here the pinched cylinder with diaphragms) and then we propose an application of solid shell elements for the static analysis of a concrete structure which is a particular cell of a shallow foundation system called Spider Net System Footing. In all examples the good behaviour of both solid shell elements is observed with a faster convergence using the DKMQ-SS element.

5. REFERENCES

[1] K.J. Bathe, E.N. Dvorkin, A formulation of general shell elements- the use of mixed interpolation of tensorial components, *Int. J. Num. Meth. Engng*, 22 (1986), pp. 697-722.

[2] J.L. Batoz, G. Dhatt, *Finite Element Modeling of Structures*, Lavoisier 1992, Paris.
[3] Katili I., Batoz J.-L., Maknun I.J., Hamdouni A., Millet O. (2014), The development of DKMQ plate bending element for thick to thin shell analysis based on Naghdi/Reissner/Mindlin shell theory, *Fin. Elem. Analysis and Design*, 100: 12-27.
[4] I. Katili, I., J.L. Batoz, I. Maknun, P. Lardeur, (2018), "A comparative formulation of DKMQ, DSQ and MITC4 quadrilateral plate elements with new numerical results based on s-norm tests", *Computer and Structures*, **204**, 48-64, 2018.
[5] K.Y. Sze, L.Q. Yao, A hybrid stress ANS solid–shell element and its generalization for smart structure modeling, Part I-solid–shell element formulation, *Int. J. Num. Meth. Engng*, 48 (2000), pp. 545-564.
[6] L. Vu-Quoc, X.G. Tan, Optimal solid shells for non-linear analyses of multilayer composites. I. Statics, *Comp. Meth. Appl. Mech. Eng.*, 192 (2003), pp. 975-1016.
[7] R.P.R. Cardoso, J.W. Yoon, M. Mahardika, S. Choudry, R.J. Alves de Sousa, R.A.F. Valente, Enhanced assumed strain (EAS) and assumed natural strain (ANS) methods for one-point quadrature solid-shell elements, *Int. J. Num. Meth. Engng,* 75 (2008), pp. 156-187.
[8] M. Schwarze, S. Reese, A reduced integration solid-shell finite element based on the EAS and the ANS concept—geometrically linear problems, *Int. J. Num. Meth. Engng,* 80 (2009), pp. 1322-1355.
[9] R.A.S. Moreira, R.J. Alves de Sousa, R.A.F. Valente, A solid-shell layerwise finite element for non-linear geometric and material analysis, *Compos. Struct.*, 92 (6) (2010), pp. 1517-1523.
[10] B. Bassa, F. Sabourin, M. Brunet, A new nine-node solid-shell finite element using complete 3D constitutive laws, *Int. J. Num. Meth. Engng.*, 92 (7) (2012), pp. 589-636.
[11] K. Rah, W. Van Paepegem, A.M. Habraken, J. Degrieck, J.R. Alves de Souza, R.A.F. Valente, Optimal low-order fully integrated solid-shell elements, *Comput. Mech.*, 2012, DOI 10.1007/s00466-012-0726-6
[12] H. Naceur, S. Shiri, D. Coutellier and J.L Batoz, On the modeling and design of composite multilayered structures using solid-shell finite element model, *Fin. Elem. Analysis and Design*, Vol. 70, 1-14, 2013.
[13] M. Mostafa, M.V. Sivaselvan, C. Felippa, A solid-shell corotational element based on ANDES, ANS and EAS for geometrically nonlinear structural analysis, *Int. J. Numer. Meth. Engng*, 2013, 95:145-180.
[14] https://www.altairhyperworks.com/
[15] https://www.3ds.com/fr/produits-et-services/simulia/produits/abaqus/abaqusstandard/
[16] Darjanto H, Irsyam M, Retno S.R, "Full Scale Load Test on The Spider Net System", Jurnal Teknologi (Sciences & Engineering), Universiti Teknologi Malaysia, vol.77, no 11, 73-82, 2015.
[17] Soelarso, Antaluca E, Batoz, J.L, Lamarque F, On the finite element bearing capacity analysis of a rib system to be used as shallow foundation construction, *IOP Conf. Ser.: Mater. Sci. Eng.* 673 011002, 2019 (BEST 2019).
[18] 2019 *IOP Conf. Ser.: Mater. Sci. Eng.* **673** 011002